Bioorganic & Medicinal Chemistry 16 (2008) 8196–8204

Contents lists available at ScienceDirect

Bioorganic & Medicinal Chemistry

journal homepage: www.elsevier.com/locate/bmc

Antibacterial profile against drug-resistant *Staphylococcus epidermidis* clinical strain and structure–activity relationship studies of 1*H*-pyrazolo[3,4-*b*]pyridine and thieno[2,3-*b*]pyridine derivatives

Bruno Leal [a], Ilídio F. Afonso [b], Carlos R. Rodrigues [b,*], Paula A. Abreu [a], Rafael Garrett [a], Luiz Carlos S. Pinheiro [c], Alexandre R. Azevedo [c], Julio C. Borges [c], Percilene F. Vegi [c], Cláudio C. C. Santos [d], Francisco C. A. da Silveira [a], Lúcio M. Cabral [b], Izabel C. P. P. Frugulhetti [a], Alice M. R. Bernardino [c], Dilvani O. Santos [a], Helena C. Castro [a,*]

[a] *Universidade Federal Fluminense, Instituto de Biologia, Departamento de Biologia Celular e Molecular, LABioMol, 24210-130 Niterói, RJ, Brazil*
[b] *Universidade Federal do Rio de Janeiro, Faculdade de Farmácia, ModMolQSAR, 24020-150 Rio de Janeiro, RJ, Brazil*
[c] *Universidade Federal Fluminense, Instituto de Química, Departamento de Química Orgânica, Programa de Pós-Graduação em Química Orgânica, Campus do Valonguinho 24210-150, Niterói, RJ, Brazil*
[d] *Fundação Ataulpho de Paiva, FAP, 20941-070 Rio de Janeiro, RJ, Brazil*

ARTICLE INFO

Article history:
Received 1 June 2008
Revised 15 July 2008
Accepted 16 July 2008
Available online 20 July 2008

Keywords:
Antimicrobial activity
Antibacterial activity
Pyrazolopyridine
MIC
Staphylococcus epidermidis
Structure–activity relationship (SAR)
In silico ADMET screening

ABSTRACT

Antibacterial resistance is a complex problem that contributes to health and economic losses worldwide. The *Staphylococcus epidermidis* is an important nosocomial pathogen that affects immunocompromised patients or those with indwelling devices. Currently, there are several resistant strains including *S. epidermidis* that became an important medical issue mainly in hospital environment. In this work, we report the biological and theoretical evaluations of a 4-(arylamino)-1-phenyl-1*H*-pyrazolo[3,4-*b*]pyridine-5-carboxylic acids series (**1, 1a–m**) and the comparison with a new isosteric ring nucleus series, 4-(arylamino)thieno[2,3-*b*]pyridine-5-carboxylic acids derivatives (**2, 2a–m**). Our results revealed the 1*H*-pyrazolo[3,4-*b*]pyridine derivatives significant antibacterial activity against a drug-resistant *S. epidermidis* clinical strain in contrast to the thieno[2,3-*b*]pyridine series. The minimal inhibitory concentration (MIC) of the most active derivatives (**1a, 1c, 1e**, and **1f**) against *S. epidermidis* was similar to that of oxacillin and twofold better than chloramphenicol. Interestingly, the position of the functional groups has a great impact on the activity as observed in our structure–activity relationship (SAR) study. The SAR of 1*H*-pyrazolo[3,4-*b*]pyridine derivatives shows that the highest inhibitory activity is observed when the *meta* position is occupied by electronegative substituents. The molecular modeling analysis of frontier molecular orbitals revealed that the LUMO density is less intense in *meta* than in *ortho* and *para* positions for both series (**1** and **2**), whereas HOMO density is overconcentrated in 1*H*-pyrazolo[3,4-*b*]pyridine ring nucleus compared to the thieno[2,3-*b*]pyridine system. The most active derivatives of series **1** were submitted to in silico ADMET screening, which confirmed these compounds as potential antibacterial candidates.

1. Introduction

The global threat of antimicrobial resistance is a serious matter under review by the WHO and many countries throughout the world.[1–4] Currently, the widespread selective pressure and the efficient dissemination channels for multidrug-resistant organisms are major factors that may have contributed to the rapid emergence of the resistant organisms.[1–5]

Staphylococcus epidermidis is among the most compromising resistant strains.[4–6] This Gram-positive bacterium is a major component of the normal human biota, and is recognized as an important nosocomial pathogen affecting immunocompromised patients or those with indwelling devices (i.e., joint prostheses, prosthetic heart valves, and central venous catheters). The resistant strains complicate the treatment, and extremely affect the recovery of patients.[4–6]

Fused heterocyclic containing pyrazolopyridine systems have been described associated with several biological and medicinal activities including anxiolytic,[7] antiviral,[8,9] antileishmanial,[10] and anti-inflammatory[11] profiles. In particular, thieno-pyridines are of special importance due to the reported biological activities,[12]

* Corresponding authors. Tel.: +55 21 25626444 (C.R.R.); +55 21 26292294 (H.C.C.).
E-mail addresses: rangel@pharma.ufrj.br (C.R. Rodrigues), hcastrorangel@vm.uff.br, hcastrorangel@yahoo.com.br (H.C. Castro).

0968-0896/$ - see front matter © 2008 Elsevier Ltd. All rights reserved.
doi:10.1016/j.bmc.2008.07.035

including antibacterial,[13] anti-inflammatory,[14] antiviral,[15] and antiparasitic[16] profiles.

Although the importance of ring systems in the drug discovery process is recognized, the current bioactive molecules described in literature include a limited number of unique ring types. In this work, we have employed a bioisosteric design to get additional insights into the importance of different ring systems on the antibacterial profile. Literature points this approach for not only getting molecules with better bioavailability/selectivity and easier to synthesize but also replacing patented structural features.[17,18]

Herein we compared 4-(arylamino)-1-phenyl-1*H*-pyrazolo[3,4-*b*]pyridine-5-carboxylic acids (**1, 1a–m**) derivatives with a new isosteric ring nucleus series, the 4-(arylamino)thieno[2,3-*b*]pyridine-5-carboxylic acids (**2, 2a–m**) derivatives. Thus, the present study reports the synthesis, the antibacterial profile against a drug-resistant *S. epidermidis* clinical strain, and the structure–activity relationship (SAR) evaluation of both series (**1–2**). In the SAR studies, the biological properties of these molecules were compared with several theoretical parameters such as dipole moment, E_{Homo}, E_{Lumo}, c log *P*, and molecular electrostatic potential map (MEP) calculated using a molecular modeling approach. In addition the distribution of HOMO and LUMO over the ring core was analyzed as this feature may be related to the interaction of the molecule with the target receptor. Since the compounds are considered for oral delivery, they were also submitted to the analysis of Lipinski Rule of Five.[19] Finally the compounds' toxicity was experimentally and theoretically evaluated to determine their potential as safe leading compounds.

2. Results and discussion

2.1. Chemistry

2.1.1. Chemistry of 4-(arylamino)-1-phenyl-1*H*-pyrazolo[3,4-*b*]pyridine-5-carboxylic acids (1, 1a–m) and 4-(arylamino)thieno[2,3-*b*]pyridine-5-carboxylic acids (2, 2 a–m) derivatives

The synthesis of 4-(arylamino)-1-phenyl-1*H*-pyrazolo[3,4-*b*]pyridine-5-carboxylic acids (**1, 1a–m**) derivatives was performed in high yields (86–93%) by using a modified process reported elsewhere.[8–10,20]

The synthesis of 4-(arylamino)-1-phenyl-1*H*-pyrazolo[3,4-*b*]pyridine-5-carboxylic acids (**1, 1a–m**) was achieved with an efficient synthetic route (Scheme 1). Ethyl 4-chloro-1-phenyl-1*H*-pyrazolo[3,4-*b*]pyridine-5-carboxylate **(4)** was available in our laboratory, and could be easily prepared[8–10,20] from 5-aminopyrazoles through condensation with diethyl ethoxymethylenemalonate followed by 'chlorocyclization' with phosphorous oxychloride. Ethyl 4-chloro-1-phenyl-1*H*-pyrazolo[3,4-*b*]pyridine-5-carboxylate **(4)** on fusion with appropriate substituted anilines generated the required ethyl 4-(arylamino)-1-phenyl-1*H*-pyrazolo[3,4-*b*]pyridine-5-carboxylates **(3, 3a–m)** in yields 68–64%, respectively. Subsequent hydrolysis of **3** and **3a–m** afforded the corresponding 4-(arylamino)-1-phenyl-1*H*-pyrazolo[3,4-*b*]pyridine-5-carboxylic acids **(1, 1a–m)** in high yields, 93–86%, respectively.

The design of the 4-(arylamino)thieno[2,3-*b*]pyridine-5-carboxylic acids (**2, 2a–m**) was based in the substitution of the 1*H*-pyrazolo[3,4-*b*]pyridine ring by the thieno[2,3-*b*]pyridine, an isosteric ring nucleus, in the **1** series (Fig. 1). The synthesis of this new series was performed with yield of 65–75% by using a modified process reported elsewhere (Scheme 1).[15,16] The synthesis of 4-(arylamino)thieno[2,3-*b*]pyridine-5-carboxylic acids **(2, 2a–m)** was outlined in Scheme 1. The derivative 4-chlorothieno[2,3-*b*]pyridine-5-carbonitrile **(5)** was prepared from 2-aminothiophene through condensation with ethyl (ethoxymethylene)cyanoacetate to produce ethyl α-cyano-β-(*N*-2-thienylammonium)acrylate yielding 88%. The cyclization of acrylate was carried out by refluxing it in dowtherm (250 °C) for 40 min and affording the 4-hydroxythieno[2,3-*b*]pyridine-5-carbonitrile with 78% yield. The compound 4-hydroxythieno[2,3-*b*]pyridine-5-carbonitrile was easily chlorinated in refluxing phosphorous oxychloride, affording 4-chlorothieno[2,3-*b*]pyridine-5-carbonitrile **(5)** with 76% yield. For producing the derivatives 4-(arylamino)thieno[2,3-*b*]pyridine-5-carbonitrile **(6, 6a–m)**, an equimolar mixture of appropriate substituted anilines was heated, without solvents, for 4 h at 140 °C producing the compounds, **(6, 6a–m)**, with yields of 93–86%.[15,16]

A solution of 4-(arylamino)thieno[2,3-*b*]pyridine-5-carbonitriles **(6, 6a–m)** in 6 N HCl was heated for 24 h. On cooling, the mixture was alkalinized with 10% NaOH solution, and the precipitates was filtered and recrystallized from a mixture of ethanol and water.[21]

2.2. Biological evaluation (microbiology and cytotoxicity)

2.2.1. Antibacterial susceptibility tests (ASTs)

The initial screening was performed using 5 mg/mL of the (**1a–m**) and thieno[2,3-*b*]pyridine (**2a–m**) derivatives in the ASTs as described in Section 4. Although both series included unsubstituted (**1** and **2**), *meta* (**1a–f** and **2a–f**), and *para*-substituted (**1g–m** and **2g–m**) derivatives, the antibacterial analysis against the drug-resistant *S. epidermidis* clinical strain showed only *meta*-substituted 1*H*-pyrazolo[3,4-*b*]pyridine derivatives (**1a–f** and **1l**) with

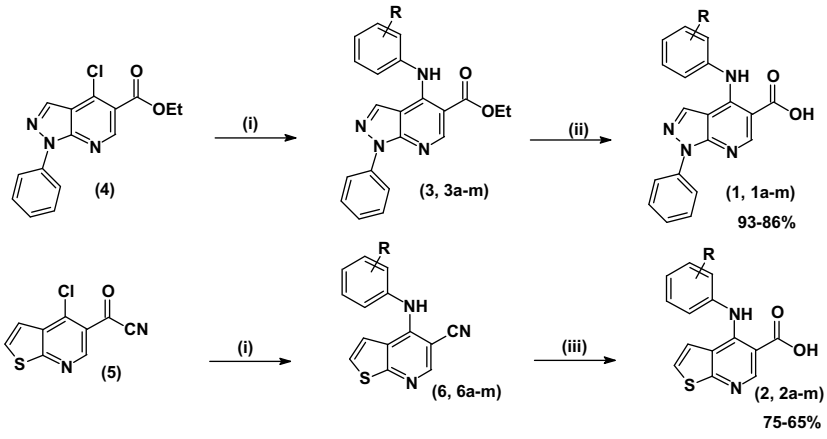

Scheme 1. Reagents and conditions: (i) anilines, 140 °C, 4 h; (ii) NaOH 20%, reflux, 3 h; (iii) HCl 6 N, reflux, 24 h.

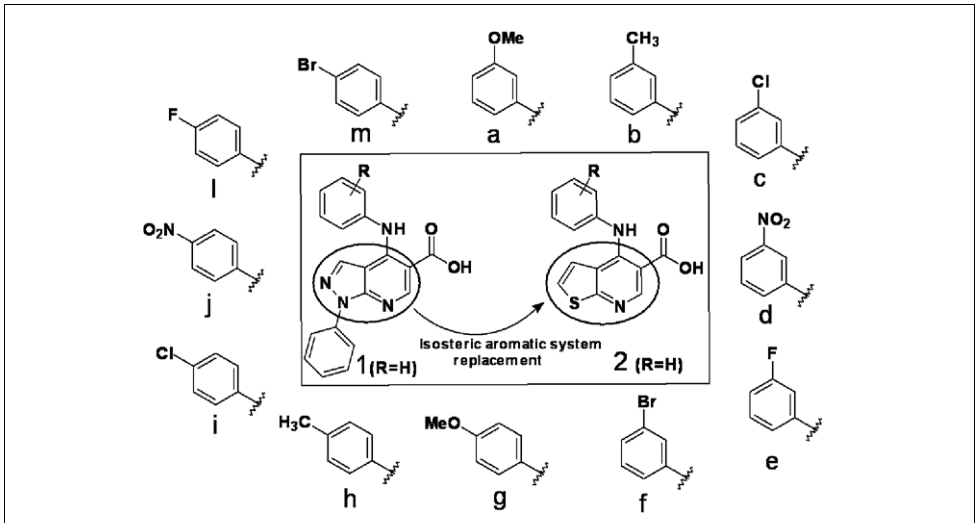

Comp	R	Halo (mm)	MIC (μg/mL)	CC[a] (%)	E_{HOMO}	E_{LUMO}	Dipole (debye)	Lipinski rule				
								cLogP	HBA	HBD	MW	PSA (Å²)
1	H	0	ND	91	-5.82	-1.50	1.33	3.28	5	2	330.35	58.49
1a	*m*-OCH_3	15	16	100	-5.78	-1.47	2.45	3.15	6	2	360.37	65.59
1b	*m*-CH_3	16	64	100	-5.78	-1.45	1.73	3.76	5	2	344.37	58.49
1c	*m*-Cl	17	16	100	-5.96	-1.67	1.20	3.83	5	2	364.79	58.48
1d	*m*-NO_2	12	ND	100	-6.17	-2.43	4.51	3.31	8	2	375.34	97.18
1e	*m*-F	20	16	100	-5.94	-1.70	1.18	3.43	5	2	348.34	59.65
1f	*m*-Br	17	16	100	-5.97	-1.68	1.27	4.11	5	2	409.24	58.43
1g	*p*-OCH_3	0	ND[b]	100	-5.69	-1.29	2.50	3.15	6	2	360.37	65.73
1h	*p*-CH_3	0	ND	100	-5.76	-1.32	2.23	3.76	5	2	344.37	58.53
1i	*p*-Cl	0	ND	100	-5.87	-1.47	1.73	3.83	5	2	364.79	58.18
1j	*p*-NO_2	0	ND	88	-6.26	-2.41	5.52	3.31	8	2	375.34	97.24
1l	*p*-F	0	ND	100	-5.86	-1.58	0.72	3.43	5	2	348.34	58.47
1m	*p*-Br	10	ND	92	-5.91	-1.77	1.22	4.11	5	2	409.24	59.39
2	H	0	ND	100	-5.78	-1.56	2.89	2.97	4	2	270.31	46.27
2a	*m*-OCH_3	0	ND	100	-5.69	-1.60	1.82	2.85	5	2	300.34	53.20
2b	*m*-CH_3	0	ND	100	-5.74	-1.52	3.12	3.46	4	2	284.34	46.28
2c	*m*-Cl	0	ND	100	-5.88	-1.59	2.93	3.53	4	2	304.76	46.14
2d	*m*-NO_2	0	ND	100	-6.21	-2.33	4.45	3.01	7	2	315.31	84.15
2e	*m*-F	0	ND	100	-5.84	-1.55	2.79	3.13	4	2	288.30	46.20
2f	*m*-Br	0	ND	100	-5.89	-1.60	2.93	3.80	4	2	349.21	46.20
2g	*p*-OCH_3	0	ND	100	-5.54	-1.29	3.83	2.85	5	2	300.34	53.29
2h	*p*-CH_3	0	ND	100	-5.65	-1.35	3.55	3.46	4	2	284.34	46.33
2i	*p*-Cl	0	ND	100	-5.85	-1.58	1.36	3.53	4	2	304.76	46.22
2j	*p*-NO_2	0	ND	100	-6.34	-2.35	4.04	3.01	7	2	315.31	84.12
2l	*p*-F	0	ND	100	-5.79	-1.46	1.93	3.13	4	2	288.30	46.32
2m	*p*-Br	0	ND	100	-5.86	-1.60	1.32	3.80	4	2	349.21	46.23

[a]Cytotoxicity (%) represented by cellular viability at 700μM of the compounds
[b]Not detected.

Figure 1. Comparison of the antibacterial profile against a drug-resistant *Staphylococcus epidermidis* clinical strain (antibacterial susceptibility test—halo, minimal inhibitory concentration—MIC), cytotoxicity on peripheral blood mononuclear cells (CC), and theoretical parameters (E_{HOMO}, E_{LUMO}, dipole moment, and Lipinski Rule of Five) of the series of 4-(arylamino)-1-phenyl-1*H*-pyrazolo[3,4-*b*]pyridine-5-carboxylic acids (**1**, **1a**–**m**) and 4-(arylamino)thieno[2,3-*b*]pyridine-5-carboxylic acids (**2**, **2 a**–**l**).

an active biological profile (halo = 10–20 mm) (Fig. 1). No antibacterial activity was observed when using other drug-resistant Gram-positive and Gram-negative clinical bacteria (not shown), which suggested a specific mechanism against *S. epidermidis*. Overall these screening tests showed the potential of 1*H*-pyrazolo[3,4-*b*]pyridine system as an antibacterial lead structure against the drug-resistant *S. epidermidis* clinical strain in contrast to the thieno[2,3-*b*]pyridine system. In addition the *meta* position in the 1*H*-pyrazolo[3,4-*b*]pyridine series was also pointed as an important structural feature to this specific biological profile.

2.2.2. Minimal inhibitory concentration (MIC) assays

The MIC assays of the active compounds (**1a–e** and **1f**) showed all with an antibacterial profile (MIC = 16 μg/mL) in the range of antibiotics current on the market (MIC = 1–40 μg/mL), except for **1b** that presents a methyl group at *meta* position (MIC = 64 μg/mL) (Figs. 1 and 2). The comparison showed that these compounds are similar to oxacillin and are better than chloramphenicol, both clinical antibiotics are currently in use (Fig. 2). These results reinforced the potential of these derivatives against the drug-resistant *S. epidermidis* clinical strain.

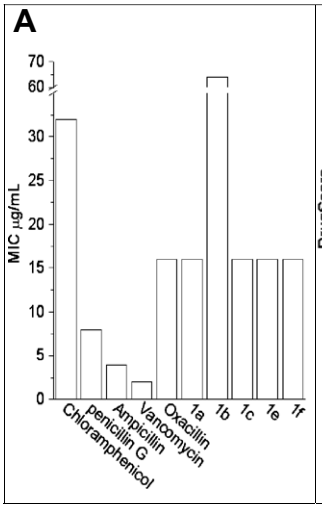

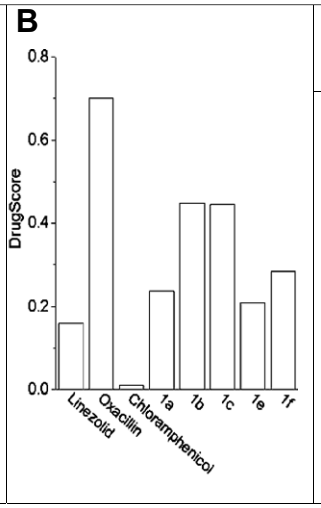

C

Drug	Toxicity effects			
	M	T	I	R
1a	medium	low	low	high
1b	low	low	low	low
1c	low	low	low	low
1d	medium	medium	low	low
1e	low	low	low	medium
1f	low	low	low	low
oxacillin	low	low	low	low
penicillin G	low	low	low	low
chloramphenicol	high	high	low	high
ampicillin	low	low	low	low
linezolid	high	high	low	low

Figure 2. Comparison of the most active 1*H*-pyrazolo[3,4-*b*]pyridine derivatives (**1a**, **1b**, **1c**, **1e**, and **1f**) with the clinical antibiotics currently in use. (A) Minimal Inhibitory concentration (MIC), (B) drugscore, and (C) in silico toxicity risks. M, mutagenic; T, tumorigenic; I, irritant; R, reprodutive.

2.2.3. Effects on the bacterial growth

Since all active compounds are *meta* substituted, this infers that not only the 1*H*-pyrazolo[3,4-*b*]pyridine but also the substituent position in the phenyl ring is biologically relevant. Then to analyze the importance of the substituent position in these derivatives we synthesized an *ortho*-F substituted 1*H*-pyrazolo[3,4-*b*]pyridine derivative (**1n**) to compare with *meta*-F (**1e**) and *para*-F (**1l**) derivatives on drug-resistant *S. epidermidis* clinical strain growth assays (Fig. 3). The substituent (F) was selected due to its small size and low electronic profile. Interestingly, our antibacterial data confirmed the importance of the restricted position in the ring for this biological activity since only *meta*-F (**1e**) showed an antibacterial profile in contrast to both *para*-F (**1l**) and *ortho*-F (**1n**) substituted molecules that were inactive (Fig. 3).

2.2.4. Cytotoxicity assays

To verify the cytotoxicity profile of the active compounds, we analyzed their profile against peripheral blood mononuclear cells (PBMCs). Interestingly our experimental results pointed **1a, 1c, 1e**, and **1f** as low risk compounds as the concentration used was at least 15 times higher than the MIC with no toxicity on PBMCs at 700 μM (Fig. 1). These results were similar to that observed for antibiotics currently in use in the market (oxacillin, chloramphenicol, ampicillin, and vancomycin), which kept 100% of PBMCs viability at 700 μM (not shown). In addition these data were congruent with previous results obtained with other 1*H*-pyrazolo[3,4-*b*]pyridine derivatives,[8–10] which reinforced 1*H*-pyrazolo[3,4-*b*]pyridine nucleus as a low cytotoxic structure.

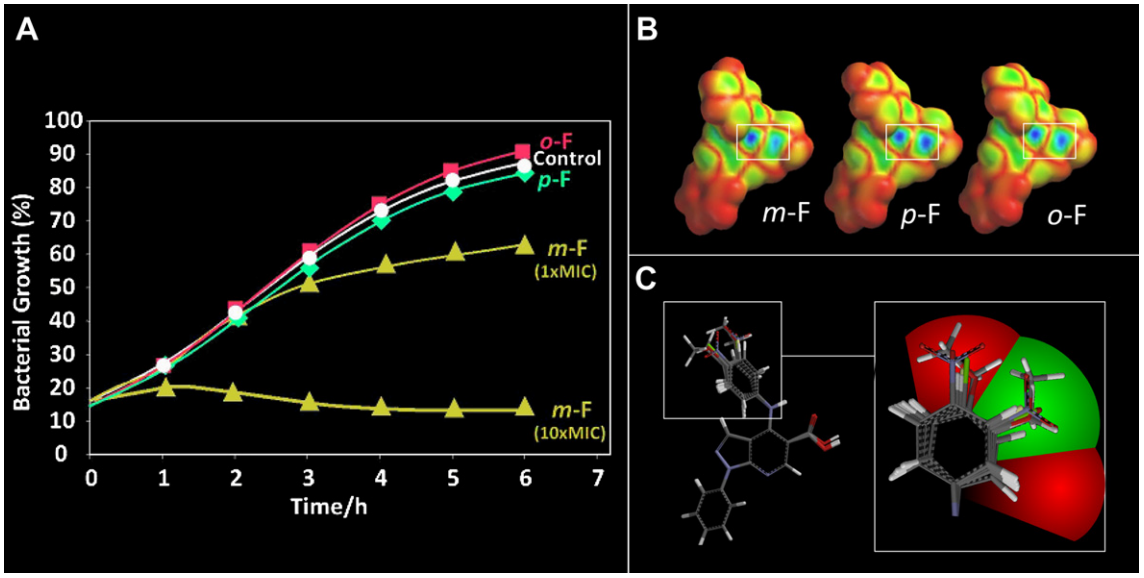

Figure 3. Comparison of *para* (*p*-F), *ortho* (*o*-F), and *meta* (*m*-F) fluoride substituted 1*H*-pyrazolo[3,4-*b*]pyridine derivatives. (A) Effects on *Staphylococcus epidermidis* growth ($p < 0.05$) of (*para*-F, *ortho*-F) substituted derivatives, tested at 5 mg/mL and *meta*-F tested at 16 μg/mL (1× MIC) and 160 μl/mL (10× MIC). (B) LUMO density encoded onto an isosurface of the 0.002 e/au^3 revealing the different degree of LUMO density distribution marked in the white box. (C) Structural alignment of all 1*H*-pyrazolo[3,4-*b*]pyridine derivatives showing a green zone allowed by the *meta* position, whereas the red zone is the prohibited zone represented by the *para and ortho* positions in the benzene ring.

2.3. Molecular modeling and SAR studies of 1*H*-pyrazolo[3,4-*b*]pyridine and thieno[2,3-*b*]pyridine systems

In this work, the structural and electronic properties of the compounds were evaluated to identify their role in modulating the 1*H*-pyrazolo[3,4-*b*]pyridine and thieno[2,3-*b*]pyridine biological profile. Initially we calculated HOMO and LUMO energy, dipole moment, and clog*P* of the derivatives that showed no clear or direct correlation with antibacterial activity (Fig. 1). These data pointed out that these parameters may not be used for establishing a feasible relationship between these compounds structures and the biological activity observed herein.

The molecular electrostatic potential map (MEP) energy isosurfaces is an alternative approach for understanding the electrostatic contribution on binding of receptor and drugs.[9] The MEP analysis of both series revealed a higher electronic density over 1*H*-pyrazolo[3,4-*b*]pyridine nucleus than that observed in the thieno-pyridine bioisosteric ring (Fig. 4). The SAR studies of **1** series MEPs suggested that the electron density concentrated in the substituted phenyl ring apparently rules the activity profile of these systems (i.e., **1b)** (Fig. 4). Meanwhile derivatives **1a, 1c, 1e**, and **1f** containing electronegative atoms as substituents (methoxy, chlorine, fluorine, and bromine, respectively) showed better biological results than **1b**, which inferred that the methyl low electronic contribution in **1b** may avoid important interactions with the receptor compared with the other active compounds (Fig. 4). Importantly, the electron withdrawing meta nitro substituent caused a significant modification on the MEP profile at the substituted phenyl ring (Fig. 4). The nitro group is a strongly deactivating group, and also led to a shift of the LUMO to the same region compared to the other derivatives (Fig. 4), which apparently compromised the activity despite its *meta* location.

Our theoretical study using HOMO depicted as a map of the orbital coefficient onto the van der Waals surface of the compounds (red = low to blue = high HOMO density) showed a higher electron density significantly concentrated over 1*H*-pyrazolo[3,4-*b*]pyridine nucleus compared to thieno[2,3-*b*]pyridine system (Fig. 4). This feature pointed out this region as feasible for maintaining π–π stacking interactions with the target.

The evaluation of the electron density/LUMO encoded onto an isosurface of 0.002 e/au^3 showed the thieno[2,3-*b*]pyridine system with an intense blue color (high orbital density) over the carboxylate group, different from 1*H*-pyrazolo[3,4-*b*]pyridine system (Fig. 4). Our results also showed differences on LUMO density among the active derivative **1e** (*meta*-F) that presented the lowest density, and the inactive derivatives **1l** (*para*-F) and **1n** (*ortho*-F) (Fig. 3).

The comparison of the structural alignment of the most active derivatives (**1a–f**) with other substituted compounds of **1** series suggested a steric hindrance when these substituents are at *para* and *ortho* positions of the phenyl ring, probably creating a prohibitive (red) zone for the antibacterial profile (Fig. 3). In fact the conformational analysis of the *meta*-substituted derivatives revealed one local energy minima where the best conformer of each *meta* compound was 10 kcal/mol more stable when the substituent was near from the pyrazole ring (not shown). This is probably caused by the hydrogen bond formed between the NH (donor) of the 1*H*-pyrazolo[3,4-*b*]pyridine system and the oxygen atom (acceptor) of the carboxylate group in this specific conformation, noticed only when the structure presents a *meta* substitutent (not shown). Thus, the more stable *meta* conformation probably allows the correct orientation of the substituent in the active derivatives for interacting in a perfect match with the *S. epidermidis* target.

The analysis of some structural properties (molecular weight, number of hydrogen bond acceptors—*n*HBA, number of hydrogen bond donors—*n*HBD, and topological surface area—tpsa) of the two series revealed that the 1*H*-pyrazolo[3,4-*b*]pyridine system presented higher values of lipophilicity, weight, *n*HBA, and tpsa than thieno[2,3-*b*]pyridine compounds (Fig. 1). As only the 1*H*-pyrazolo[3,4-*b*]pyridine compounds presented an antibacterial profile, it seems that these structural and electronic features may be important for the permeation across membranes and for the

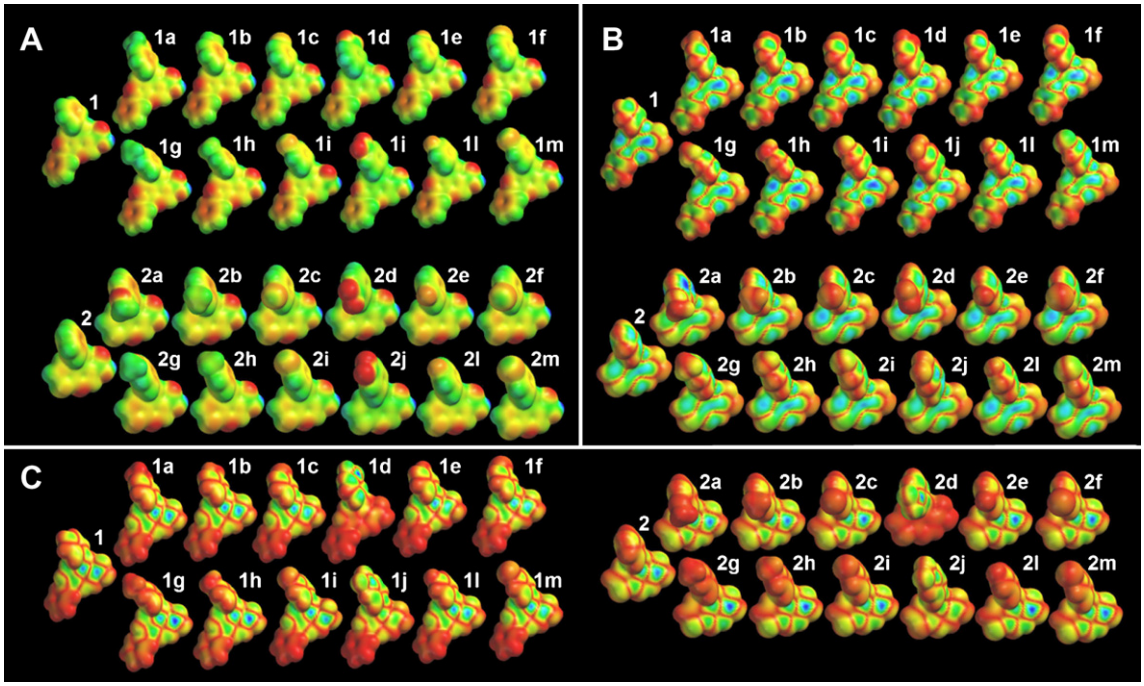

Figure 4. Electronic properties of 1*H*-pyrazolo[3,4-*b*]pyridine (**1**–**1l**) and thieno[2,3-*b*]pyridine (**2**–**2l**) derivatives. (A) Molecular electrostatic potential energy isosurfaces (MEP) superimposed onto total electrons density of 0.002 e/au^3. The color code is in the range of −25 (deepest red) to +55 kcal/mol (deepest blue). (B) HOMO, and (C) LUMO densities encoded onto a van der Waals surface (isodensity 0.002 e/au^3), the orbital absolute density coefficient was mapped from deepest red (0.00) to deepest blue (0.01).

interaction through interatomic contacts and interface complementarity with the *S. epidermidis* target.

In this work, we submitted the active compounds to the analysis of Lipinski Rule of Five that indicates if a chemical compound could be an orally active drug in humans. The rule states that most 'drug-like' molecules have c log*P* ⩽ 5, molecular weight (MW) ⩽ 500, PSA ⩽ 140, and number of hydrogen bond acceptors ⩽10 and donors ⩽5. Molecules violating more than one of these rules may have problems with bioavailability (Lipinski, 2001). Our results showed that all active compounds (**1a, 1b, 1c, 1e**, and **1f**) fulfilled this rule (molecular weight = 344.37–409.24, c log*P* = 3.15–4.11, *n*HBA = 6–7, and *n*HBD = 2) (Fig. 1), similarly to commercial drugs (*i.e.* chloramphenicol, oxacillin, ampicillin, penicillin G, and linezolid) (not shown).

Currently there are many approaches that assess a compound drug-likeness based on topological descriptors, fingerprints of molecular drug-likeness structure keys or other properties such as c log*P* and molecular weight.[22] In the Osiris program (http://www.organic-chemistry.org/prog/peo) the occurrence frequency of each fragment is determined within the collection created by shreddering 3300 traded drugs as well as 15,000 commercially available chemicals (Fluka) yielding a complete list of all available fragments. In this case, positive values point out that the molecule contains predominantly the better fragments, which are frequently present in commercial drugs but not in the non-drug-like collection of Fluka compounds. In this work, we used the Osiris program for calculating the fragment based drug-likeness of the active compounds also comparing them with penicillin G, chloramphenicol, oxacillin, ampicillin, and linezolid (Fig. 4).

Interestingly, the derivatives **1a, 1b, 1c, 1e**, and **1f** presented better drug-likeness values (from −3.68 to −0.12) than chloramphenicol (−4.61) and linezolid (−4.08) (not shown). In this study we also verified the drugscore, which combines drug-likeness, c log*P*, log*S*, molecular weight, and toxicity risks in one value and this may be used to judge the compound's overall potential to qualify for a drug.[23] Our theoretical data showed that **1a–f** derivatives presented values once again higher than chloramphenicol and linezolid (Fig. 2).

Drug toxicity is a factor of great importance for a potential commercial drug, since a significant number of drugs are disapproved in clinical trials based on their high toxicity profile. Herein, we used the Osiris program (Fig. 2) to predict the overall toxicity of the most active derivatives as it may point to the presence of some fragments generally responsible for the irritant, mutagenic, tumorigenic, or reproductive effects in these molecules. Interestingly, most of the active derivatives presented a low in silico toxicity risk profile, similar to oxacillin, ampicillin, and penicillin G, and even lower than that observed for chloramphenicol and linezolid (Fig. 2). These theoretical data reinforced the cytotoxicity experimental data described in this work pointing these compounds as lead compounds with low cytotoxicity.

3. Conclusion

In this work, we synthesized 26 4-(arylamino)-1-phenyl-1*H*-pyrazolo[3,4-*b*]pyridine-5-carboxylic acids (**1**, **1a–m**) and 4-(arylamino)thieno[2,3-*b*]pyridine-5-carboxylic acids (**2**, **2a**–**m**) derivatives to evaluate their antibacterial profile and to correlate the biological results with some molecular properties. The study revealed new four lead 1*H*-pyrazolo[3,4-*b*]pyridine compounds with significant antibacterial activity on a drug-resistant *S. epiderrmidis* clinical strain, similar to oxacillin, and are twofold better than chloramphenicol. Interestingly, the 1*H*-pyrazolo[3,4-*b*]pyridine system and the position of functional groups have a great impact on the activity as observed in the SAR study. The highest inhibitory activity is noticed when (a) the *meta* position is occupied by electronegative substituents and (b) the 1*H*-pyrazolo[3,4-*b*]pyridine derivatives present higher HOMO electron density. The active compounds also showed low experimental and theoretical toxicity, and were theoretically feasible as orally active drugs in humans as they fulfilled the Lipinski Rule of Five. These new lead compounds and the analyses of their molecular properties may be useful for designing new and more efficient antibacterial drugs for fighting the emergence of new resistant bacterial strains, an important issue for public health that still lies ahead.

4. Experimental

4.1. Chemistry

All reagents and solvents used were of analytical grade. The ^{1}H Nuclear Magnetic Resonance (NMR) spectra were obtained on a 300 MHz, Varian Unity Plus instrument using tetramethylsilane as internal standard. The chemical shifts (δ) are reported in ppm and the coupling constants (J) in Hertz. Fourier transform infrared (FT-IR) spectra were recorded in a Perkin-Elmer Spectrum One FT-IR. The solid samples were determined in potassium bromide (KBr) pellets. Melting points (mp) were determined with a Fisher–Johns apparatus. TLC was carried out using silica gel F-254 Glass Plate (20 × 20 cm). All reagents and solvents used were of analytical grade. The EI-MS spectra were recorded using a Finingan MAT 711 A instrument. The ionization energy was 70 eV with the source 200 °C and an accelerative voltage of 8 kV. Samples were introduced by the standard direct insertion probe. High-resolution data were obtained with the instrument using 10,000 resolution.

4.1.1. General procedure for synthesis of the 4-(arylamino)-1-phenyl-1H-pyrazolo[3,4-*b*]pyridines (1, 1a–m)

A mixture of the derivatives **(3, 3a–m)** (2 mmol), 10 mL of 20% sodium hydroxide solution, and 10 mL of ethanol was heated under reflux for 1–3 h. On cooling the mixture was acidified with diluted hydrochloric acid (1:3), and the precipitated acids were filtered and recrystallized from a mixture of DMF and water.[8–10,20]

4.1.1.1. 4-Phenylamino-l-phenyl-1*H*-pyrazolo[3,4-*b*]pyridine-5-carboxylic acid. Yield: 86%, mp 229 °C; IR (KBr, cm^{-1}): (ν OH 3435–2598; ν C—O 1654); ^{1}H NMR (300 MHz, DMSO-d_6, TMS, J in Hz, δ in ppm) 7.01 (s, H3, 1H), 9.02 (s, H6, 1H), 8.23 (d, 8.1, H-2′,6′, 2H), 7.86–7.45 (m, 8H), 10.78 (s, N-H); EI (70 eV) m/z (%): M$^{+\cdot}$ 330.3127 (100).

4.1.1.2. 4-(3′-Methoxyphenylamino)-l-phenyl-1*H*-pyrazolo[3,4-*b*]pyridine-5-carboxylic acid (1a). Yield: 90%, mp 237 °C; IR (KBr, cm^{-1}): (ν OH 3330–2590; ν C—O 1654); ^{1}H NMR (300 MHz, DMSO-d_6, TMS, J in Hz, δ in ppm) 6.91 (s, H3, 1H), 9.05 (s, H6, 1H), 8.27 (d, 7.5, H-2′,6′, 2H), 7.69 (dd, 7.5, H-3′,5′, 2H), 7.51 (dd, 7.5, H4′, 1H), 7.66–7.61 (m, 4H), 10.88 (s, N-H), 3.95 (s, Ar-OCH$_3$); EI (70 eV) m/z (%): M$^{+\cdot}$ 360.1237 (100).

4.1.1.3. 4-(3′-Methylphenylamino)-l-phenyl-1*H*-pyrazolo[3,4-*b*]pyridine-5-carboxylic acid (1b). Yield: 90%, mp 237 °C; IR (KBr, cm^{-1}): (ν OH 3482–2592; ν C=O 1650); ^{1}H NMR (300 MHz, DMSO-d_6, TMS, J in Hz, δ in ppm) 6.71 (s, H3, 1H), 8.95 (s, H6, 1H), 8.16 (d, 7.5, H-2′,6′, 2H), 7.60 (dd, 7.5, H-3′,5′, 2H), 7.52 (dd, 7.5, H4′, 1H), 7.44–7.32 (m, 4H), 10.81 (s, N-H), 2.21 (s, Ar-CH$_3$); EI (70 eV) m/z (%): M$^{+\cdot}$ 344.1317 (95).

4.1.1.4. 4-(3′-Chlorophenylamino)-1-phenyl-1*H*-pyrazolo[3,4-*b*]pyridine-5-carboxylic acid (1c). Yield: 93%, mp 236 °C; IR (KBr, cm^{-1}): (ν OH 3488–2766; ν C—O 1649); ^{1}H NMR (300 MHz, DMSO-d_6, TMS, J in Hz, δ in ppm) 7.01 (s, H3, 1H), 9.07 (s, H6, 1H), 8.27 (d, 7.5, H-2′,6′, 2H), 7.74–7.62 (m, 5H), 7.52 (dd, 7.5,

H4′, 1H), 7.79 (s, H2″, 1H), 10.92 (s, N-H); EI (70 eV) *m*/*z* (%): $M^{+\cdot}$ 364.0792 (100).

4.1.1.5. 4-(3′-Nitrophenylamino)-1-phenyl-1*H*-pyrazolo[3,4-*b*]pyridine-5-carboxylic acid (1d). Yield: 90%, mp 255 °C, IR (KBr, cm^{-1}): (*ν* OH 3401–2603; ν C—O l674); ^1H NMR (300 MHz, DMSO-d_6, TMS, *J* in Hz, *δ* in ppm) 7.12 (s, H3, 1H), 9.04 (s, H6, 1H), 8.22 (d, 7.5, H-2′,6′, 2H), 7.65 (dd, 7.5, H-3′,5′, 2H), 7.46 (dd, 7.5, H4′, 1H), 8.42 (s, H2″, 1H), 8.35 (d, 8.7, H4″, 1H), 7.88 (d, 8.7, H5″, 1H), 8.03 (d, 8.7, H6″, 1H), 10.99 (s, N-H); EI (70 eV) *m*/*z* (%): $M^{+\cdot}$ 375.0968 (100).

4.1.1.6. 4-(3′-Fluorophenylamino)-l-phenyl-1*H*-pyrazolo[3,4-*b*]pyridine-5-carboxylic acid (1e). Yield: 93%, mp 258 °C; IR (KBr, cm^{-1}): (*ν* OH 3412–2586; ν C—O 1675); ^1H NMR (300 MHz, DMSO-d_6, TMS, *J* in Hz, *δ* in ppm) 7.04 (s, H3, 1H), 9.08 (s, H6, 1H), 8.28 (d,7.5, H-2′,6′, 2H), 7.79–7.54 (m, 6H), 7.49 (dd,7.5, H4′, 1H), 10.98 (s, N-H); EI (70 eV) *m*/*z* (%): $M^{+\cdot}$ 348.1013 (100).

4.1.1.7. 4-(3′-Bromophenylamino)-1-phenyl-1*H*-pyrazolo[3,4-*b*]pyridine-5-carboxylic acid (1f). Yield: 90%, mp 246 °C; IR (KBr, cm^{-1}): (*ν* OH 3490–2580; ν C—O 1650); ^1H NMR (300 MHz, DMSO-d_6, TMS, *J* in Hz, *δ* in ppm) 6.65 (s, H3, 1H), 8.72 (s, H6, 1H), 7.93 (d, 7.5, H-2′,6′, 2H), 7.50–7.31 (m, 5H), 7.17 (dd, 7.5, H4′, 1H), 7.57 (s, H2″, 1H), 12.90 (s, CO_2H), 10.57 (s, N-H); EI (70 eV) *m*/*z* (%): $M^{+\cdot}$ 410.0042 (100).

4.1.1.8. 4-(4′-Methoxyphenylamino)-l-phenyl-1*H*-pyrazolo[3,4-*b*]pyridine-5-carboxylic acid (1g). Yield: 91%, mp 261 °C; IR (KBr, cm^{-1}): (*ν* OH 3430–2588; ν C = O 1654); ^1H NMR (300 MHz, DMSO-d_6, TMS, *J* in Hz, *δ* in ppm) 6.70 (s, H3, 1H), 9.03 (s, H6, 1H), 8.26 (d, 7.5, H-2′,6′, 2H), 7.69 (dd, 7.5, H-3′,5′, 2H), 7.51 (dd, 7.5, H4′, 1H), 7.28 (d, 8.7, H2″, 1H), 7.56 (s, H3″, 1H), 7.56 (d, 8.7, H5″, 1H), 7.28 (d, 8.7, H6″, 1H), 10.77 (s, N-H), 4.02 (s, Ar-OCH_3); EI (70 eV) *m*/*z* (%): $M^{+\cdot}$ 360.1245 (100).

4.1.1.9. 4-(4′-Methylphenylamino)-1-phenyl-1*H*-pyrazolo[3,4-*b*]pyridine-5-carboxylic acid (1h). Yield: 92%, mp 258 °C; IR (KBr, cm^{-1}): (*ν* OH 3430–2603; ν C—O 1654); ^1H NMR (300 MHz, DMSO-d_6, TMS, *J* in Hz, *δ* in ppm) 6.67 (s, H3, 1H), 8.95 (s, H6, 1H), 8.18 (d, 7.5, H-2′,6′, 2H), 7.61–7.40 (m, 7H), 10.73 (s, N-H), 2.47 (s, Ar-CH_3); EI (70 eV) *m*/*z* (%): $M^{+\cdot}$ 344.1336 (95).

4.1.1.10. 4-(4′-Chlorophenylamino)-l-phenyl-1*H*-pyrazolo[3,4-*b*]pyridine-5-carboxylic acid (1i). Yield: 89%, mp 268 °C; IR (KBr, cm^{-1}): (*ν* OH 3430–2603; ν C—O 1654); ^1H NMR (300 MHz, DMSO-d_6, TMS, *J* in Hz, *δ* in ppm) 6.87 (s, H3, 1H), 8.97 (s, H6, 1H), 8.17 (d, 7.5, H-2′,6′, 2H), 7.61 (dd, 7.5, H-3′,5′, 2H), 7.42 (dd, 7.5, H4′, 1H), 7.58 (d, 8.7, H2″, 1H), 7.67 (d, 8.7, H3″, 1H), 7.67 (d, 8.7, H5″, 1H), 7.58 (d, 8.7, H6″, 1H), 10.77 (s, N-H); EI (70 eV) *m*/*z* (%): $M^{+\cdot}$ 364.0782 (100).

4.1.1.11. 4-(4′-Nitrophenylamino)-1-phenyl-1*H*-pyrazolo[3,4-*b*]pyridine-5-carboxylic acid (1j). Yield: 93%, mp 256 °C; IR (KBr, cm^{-1}): (*ν* OH 3409–2603; ν C—O 1678); ^1H NMR (300 MHz, DMSO-d_6, TMS, *J* in Hz, *δ* in ppm) 7.16 (s, H3, 1H), 9.06 (s, H6, 1H), 8.23 (d, 7.5, H-2′,6′, 2H), 7.65 (dd, 7.5, H-3′,5′, 2H), 7.46 (dd, 7.5, H4′, 1H), 7.74 (d, 8.7, H2″, 1H), 8.40 (d, 8.7, H3″, 1H), 8.40 (d, 8.7, H5″, 1H), 7.74 (d, 8.7, H6″,1H), 10.98 (s, N-H); EI (70 eV) *m*/*z* (%): $M^{+\cdot}$ 375.0957 (100).

4.1.1.12. 4-(4′-Fluorophenylamino)-l-phenyl-1*H*-pyrazolo[3,4-*b*]pyridine-5-carboxylic acid (1l). Yield: 93%, mp 232 °C; IR (KBr, cm^{-1}): (*ν* OH 3487–2586; ν C—O 1649); ^1H NMR (300 MHz, DMSO-d_6, TMS, *J* in Hz, *δ* in ppm) 6.82 (s, H3, 1H), 9.06 (s, H6, 1H), 8.27 (d, 7.5, H-2′,6′, 2H), 7.57 (dd, 7.5, H-3′,5′, 2H), 7.52 (dd, 7.5, H4′, 1H), 7.71 (d, 8,1, H2″, 1H), 7.70 (dd, 8.1, H3″, 1H), 7.70 (dd, 8.1, H5″, 1H), 7.71 (d, 8.1, H6″, 1H), 10.90 (s, N-H); EI (70 eV) *m*/*z* (%): $M^{+\cdot}$ 348.0960 (100).

4.1.1.13. 4-(4′-Bromophenylamino)-1-phenyl-1*H*-pyrazolo[3,4-*b*]pyridine-5-carboxylic acid (1m). Yield: 90%, mp 265 °C; IR (KBr, cm^{-1}): (*ν* OH 3431–2580; ν C—O 1651); ^1H NMR (300 MHz, DMSO-d_6, TMS, *J* in Hz, *δ* in ppm) 6.87 (s, H3, 1H), 8.95 (s, H6, 1H), 8.16 (d, 7.5, H-2′,6′, 2H), 7.59 (dd, 7.5, H-3′,5′, 2H), 7.40 (dd, 7.5, H4′, 2H), 7.50 (d, 8.7, H2″, 1H), 7.78 (d, 8.7, H3″, 1H), 7.78 (d, 8.7, H5″, 1H), 7.50 (d, 8.7, H6″, 1H), 13.00 (s, CO_2H), 10.73 (s, N-H); EI (70 eV) *m*/*z* (%): $M^{+\cdot}$ 410.0073 (100).

4.1.2. General procedure for synthesis of new 4-(arylamino)thieno[2,3-*b*]pyridine-5-carboxylic acids (2b, 2c, 2g–m)

(a) *Acid hydrolysis.* A solution of 4-(arylamino)thieno[2,3-*b*]pyridine-5-carbonitriles **(6b, 6c, 6g–m)** (2 mmol) in 6 N HCl (5 mL) was heated under reflux for 24 h. On cooling, the mixture was alkalinized with 10% aq NaOH solution, and the precipitated was filtered and recrystallized from a mixture of ethanol and water. The compounds **(2b, 2c, 2g–m)** were isolated in good yields (72–65%).[21]

(b) *Alkaline hydrolysis.* A solution of 4-(arylamino)thieno[2,3-*b*]pyridine-5-carbonitriles **(6b, 6c, 6g–m)** (2 mmol), 2 g of potassium hydroxide pellets, and 4 mL of ethyleneglycol was heated under reflux for 24 h. On cooling the mixture was acidified with diluted HCl (1:3), and the precipitate was filtered and recrystallized from a mixture of ethanol and water. The derivatives **(2b, 2c, 2g–m)** were obtained with lower yield.

4.1.2.1. 4-(4′-Methoxyphenylamino)thieno[2,3-*b*]pyridine-5-carboxylic acid[21] (2b). Yield: 70%, mp >300 °C; IR (KBr, cm^{-1}): (*ν* OH 3200–2800, ν C—O 1672); ^1H NMR (300 MHz, DMSO-d_6, TMS, *J* in Hz, *δ* in ppm) 7.59 (d, 6.0, H2, 1H); 6.38 (d, 6.0, H3, 1H); 9.23 (s, H6, 1H); 7.39 (d, 8.7, 2H); 7.28 (d, 9.0, 2H); 3.42 (s, Ar-OCH_3); 10.45 (s, CO_2H); EI (70 eV) *m*/*z* (%): $M^{+\cdot}$ 301.0951 (100).

4.1.2.2. 4-(4′-Nitrophenylamino)thieno[2,3-*b*]pyridine-5-carboxylic acid (2c). Yield: 65%, mp >300 °C; IR (KBr, cm^{-1}): (*ν* OH 3200–2800, ν C = O 1672); ^1H NMR (300 MHz, DMSO-d_6, TMS, *J* in Hz, *δ* in ppm) 7.02 (d, 6.0, H2, 1H); 6.73 (d, 6.0, H3, 1H); 9.02 (s, H6, 1H); 8.28–7.32 (m, 4H); 9.06 (s, N-H); EI (70 eV) *m*/*z* (%): $M^{+\cdot}$ 316.0283 (100).

4.1.2.3. 4-(3′-Bromophenylamino)thieno[2,3-*b*]pyridine-5-carboxylic acid (2g). Yield: 71%, mp >300 °C; IR (KBr, cm^{-1}): (*ν* OH 3200–2800, ν C—O 1670); ^1H NMR (300 MHz, DMSO-d_6, TMS, *J* in Hz, *δ* in ppm) 7.58 (d, 6.0, H2, 1H), 6.59 (d, 6.0, H3, 1H), 9.18 (s, H6, 1H), 7.49–7.09 (m, 4H); EI (70 eV) *m*/*z* (%): $M^{+\cdot}$ 350.8931 (100).

4.1.2.4. 4-(3′-Chlorophenylamino)thieno[2,3-*b*]pyridine-5-carboxylic acid (2h). Yield: 72%, mp >300 °C; IR (KBr, cm^{-1}): (*ν* OH 3200–2800, ν C—O 1679); ^1H NMR (300 MHz, DMSO-d_6, TMS, *J* in Hz, *δ* in ppm) 7.58 (d, 6.0, H2, 1H); 6.55 (d, 6.0, H3, 1H); 8.96 (s, H6, 1H); 7.52–7.22 (m, 4H); 10.45 (s, CO_2H); EI (70 eV) *m*/*z* (%): $M^{+\cdot}$ 305.0090 (100).

4.1.2.5. 4-(3′-Fluorophenylamino)thieno[2,3-*b*]pyridine-5-carboxylic acid (2i). Yield: 67%, mp >300 °C; IR (KBr, cm^{-1}): (*ν* OH 3200–2800, ν C—O 1670); ^1H NMR (300 MHz, DMSO-d_6, TMS, *J* in Hz, *δ* in ppm) 7.81 (d, 6.0, H2, 1H), 6.33 (d, 6.0, H3, 1H), 9.19 (s, H6, 1H), 7.52–6.80 (m, 4H), 10.79; (s, CO_2H); EI (70 eV) *m*/*z* (%): $M^{+\cdot}$ 289.0360 (100).

4.1.2.6. 4-(3′-Nitrophenylamino)thieno[2,3-*b*]pyridine-5-carboxylic acid (2j). Yield: 68%, mp >300 °C; IR (KBr, cm^{-1}): (ν OH 3200–2800, ν C = O 1684); ^{1}H NMR (300 MHz, DMSO-d_6, TMS, J in Hz, δ in ppm) 7.71 (d, 6.0, H2, 1H), 6.73 (d, 6.0, H3, 1H), 9.02 (s, H6, 1H), 8.14–7.69 (m, 4H), 10.45 (s, CO_2H), EI (70 eV) m/z (%): $M^{+\cdot}$ 316.0294 (100).

4.1.2.7. 4-(3′-Methoxyphenylamino)thieno[2,3-*b*]pyridine-5-carboxylic acid (2l). Yield: 72%, mp >300 °C; IR (KBr, cm−1): (ν OH 3200–2800, ν C—O 1671); ^{1}H NMR (300 MHz, DMSO-d_6, TMS, J in Hz, δ in ppm) 7.52 (d, 6.0, H2, 1H), 6.38 (d, 6.0, H3, 1H), 9.17 (s, H6, 1H), 7.49–7.23 (m, 4H), 3.27 (s, Ar-OCH_3), 10.62 (s, CO_2H), EI (70 eV) m/z (%): $M^{+\cdot}$ 301.0389 (100).

4.1.2.8. 4-(3′-Methylphenylamino)thieno[2,3-*b*]pyridine-5-carboxylic acid (2m). Yield: 72%, mp >300 °C; IR (KBr, cm^{-1}): (ν OH 3200–2800, ν C—O 1671); ^{1}H NMR (300 MHz, DMSO-d_6, TMS, J in Hz, δ in ppm) 7.55 (d, 6.0, H2, 1H), 6.41 (d, 6.0, H3, 1H), 9.00 (s, H6, 1H), 7.47–7.18 (m, 4H), 2.44 (s, Ar-CH_3), 10.69 (s, CO_2H), EI (70 eV) m/z (%): $M^{+\cdot}$ 285.0376 (100).

4.2. Antibacterial assays

4.2.1. Bacteria

The nine drug-resistant Gram-positive (*Enterococcus faecalis* and *Staphylococcus epidermidis*) and Gram-negative (*Escherichia coli*, *Serratia marcencens*, *Proteus mirabilis*, *Pseudomonas aeruginosa*, *Enterobacter cloacae*, *Acinetobacter calcoaceticus*, and *Klebsiella pneumoniae*) clinical bacteria were isolated from patients of the Hospital Antônio Pedro from Fluminense Federal University, and were grown at 37 °C as described elsewhere.[24] All other reagents were from Sigma (St. Louis, MO). After isolation, the bacterial strains were kept frozen in 10% milk sterilized solution containing 10% glycerin until used in the antibacterial susceptibility tests (AST) and minimal inhibitory concentration (MIC) assays.

4.2.2. Antibacterial susceptibility test (AST)

The assays were performed according to the National Committee for Clinical Laboratory Standards (NCCLS), in Müeller–Hinton medium as described elsewhere[24] Briefly, the strains were grown at 37 °C in Müeller–Hinton medium, and 1 μL of the stock solution (5 mg/mL) of each derivative in dimethyl sulfoxide (DMSO) was placed in Whatman disks (5 mm diameter). The disks were put on exponentially growing plated cultures with appropriate dilution to 1.0×10^7 colony forming unit (CFU/mL), which were then incubated for 24 h at 37 °C. The inocula used in growth method were those where turbidity was equal to 0.5 McFarland Standard. The results were verified by measuring the inhibitory zones surrounding the disk. Ciprofloxacin and vancomycin were used as positive controls, and the halo >15 mm was considered the minimum value for positive antibacterial activity as it generally leads to a minimal inhibitory concentration (MIC) near that observed for the newest antibiotics which are currently present in the market (MIC = 1–40 μg/mL) using these assays. Vancomycin and ciprofloxacin presented halos ~15–17 and 23–25 mm, respectively, in the strains tested herein ($p < 0.005$).

4.2.3. Minimal inhibitory concentration assays (MIC)

MIC was determined only for active compounds on the AST by using the macro-dilution broth method. All MIC were performed in triplicate as described previously.[24] Briefly, after 5 h of the bacterial growth, the culture was diluted to obtain 1.0×10^5 colony forming unit (CFU/mL). Then each compound was added to reach a final concentration from 0.5 to 1024 μg/mL, and was incubated at 37 °C for 24 h. MIC was defined as the lowest compound concentration preventing visible bacterial growth. All strains were tested at least in duplicate in four separate experiments, and a reference antibiotic (vancomycin) was used as a positive control (MIC = 2 μg/mL).

4.2.4. Effects on the bacterial growth

The importance of the *meta*, *para*, and *ortho* positions in the phenyl ring to the antibacterial profile was determined by testing the fluoride (*meta*-F, *para*-F, and *ortho*-F) substituted derivatives effects on drug-resistant *S. epidermidis* clinical strain culture growth monitored during 6 h at 560 nm as described previously[24] Briefly, cultures in the logarithimic growth phase were incubated with the fluoride compounds at 1 and 10× MIC and 5 mg/mL. The values of optical density were presented as growth (%) compared to the control.

4.2.5. Cytotoxicity assays

Peripheral blood mononuclear cells (PBMCs) from healthy human donors were obtained by density gradient centrifugation (Hystopaque, Sigma Chem. Co, St. Louis, MO) from buffy coat preparations. Cells were resuspended in RPMI 1640 supplemented with 10% heat-inactivated fetal bovine serum (FBS, Hyclone, Logan, UT), penicillin (100 U/mL), streptomycin (100 μg/mL), 2 mM glutamine, and 10 mM Hepes, stimulated with 5 μg/mL of phytohemagglutinin (PHA, Sigma) during 2–3 days, and further maintained in culture medium containing 5 U/mL of recombinant human interleukin-2 (Sigma). After these cells were treated with several concentrations of the compounds for 3–5 days incubated in 96-multiwell plates on the conditions of 5% CO_2, at 37 °C cell viability was determined colorimetrically by the XTT method[25] In brief, 50 μl of XTT was added to wells, and the optical density (OD) was measured at 450 nm, 2 h later. All experiments were performed in duplicate at least three times of each derivative (700 μM). Oxacillin, chloramphenicol, ampicillin, vancomycin are clinical antibiotics and were used as standard (700 μM) in the assays.

4.2.6. Molecular modeling and SAR studies

The molecular modeling study was performed using SPARTAN'06 (Wavefunction Inc. Irvine, CA, 2006) and Osiris programs (http://www.organic-chemistry.org/prog/peo/druglikeness.html) as described elsewhere.[9] The conformation analysis was obtained through AM1 and angles of rotation in the range of 30/30°. Single Point Calculation in DFT/B3LYP was performed with database 6.31G*. Molecular electrostatic potential maps (MEPs), HOMO, and LUMO eigenvalues and orbital coefficients, and the molecular dipole moments were calculated. In this work, we also studied the drug-likeness and the drugscore of the compounds, which is based on topological descriptors, fingerprints of molecular drug-likeness, structural keys or other properties as c log P and molecular weights. In the case of Osiris Property Explorer (http://www.organic-chemistry.org/), the occurrence frequency of each fragment is determined within the collection of traded drugs and within the supposedly non-drug-like collection of Fluka compounds.

Since the compounds are considered for oral delivery, they were also submitted to the analysis of Lipinski Rule of Five,[19] which evaluate some properties of a compound that would make it a likely orally active drug in humans. These structural parameters were performed using Molispiration program (http://www.molinspiration.com/cgi-bin/properties).

Acknowledgments

We thank the Fundação de Amparo à Pesquisa do Estado do Rio de Janeiro (FAPERJ) fellowships of Castro H.C.C., Bernardino A.M.R.B., Borges J.C., and Pinheiro L.C.S.; Conselho Nacional de Desenvolvimento Científico e Tecnológico (CNPq), Coordenação de Aperfeiçoamento de Pessoal Docente (CAPES), and Universidade Federal Fluminense (PROPP-UFF) for the financial support.

References and notes

1. WHO—World Health Organization. Accessed in 2008 in http://www.who.int/ent.
2. Aspa, J.; Rajas, O.; de Castro, F. R. *Expert Opin. Pharmacother.* **2008**, *9*, 229.
3. Cook, A.; Foruya, E. Y.; Larson, E.; Vasquez, G.; Lowy, F. D. *Clin. Infect. Dis.* **2007**, *44*, 410.
4. Bjarnsholt, T.; Givskov, M. *Curr. Infect. Dis. Rep.* **2008**, *10*, 22.
5. Otto, M. *Curr. Top. Microbiol. Immunol.* **2008**, *322*, 207.
6. Sjölund, M.; Tano, E.; Blaser, M. J.; Andersson, D. I.; Engstrand, L. *Emerg. Infect. Dis.* **2005**, *11*, 1389.
7. Bare, T. M.; McLarem, C. D.; Campbell, D. J. B.; Firor, J. W.; Resch, J. F.; Walters, C. P.; Salama, A. I.; Meiners, B. A.; Patel, J. B. *J. Med. Chem.* **1989**, *32*, 2561.
8. Bernardino, A. M. R.; Azevedo, A. R.; Pinheiro, L. C. S.; Borges, J. C.; Carvalho, V. L.; Miranda, M. D.; Meneses, M. D. F.; Nascimento, M.; Ferreira, D.; Rebello, M. A.; Silva, V. A. G. G.; Frugulhetti, I. C. P. P. *Med. Chem. Res.* **2007**, *16*, 352.
9. Bernardino, A. M. R.; Castro, H. C.; Frugulhetti, I. C. P. P.; Loureiro, N. I. V.; Azevedo, A. R.; Pinheiro, L. C. S.; Souza, T. M. L.; Giongo, V.; Passamani, F.; Magalhães, U. O.; Albuquerque, M. G.; Cabral, L. M.; Rodrigues, C. R. *Bioorg. Med. Chem.* **2008**, *16*, 313.
10. Mello, H.; Echevarria, A.; Bernardino, A. M. R.; Canto-Cavalheiro, M.; Leon, L. L. *J. Med. Chem.* **2004**, *47*, 5427.
11. Lu, Z.; Ott, G. R.; Anand, R.; Liu, R.; Covington, M. B.; Vaddi, K.; Qian, M.; Newton, R. C.; Christ, D. D.; Trzaskos, J.; Duan, J. J. J. *Bioorg. Med. Chem. Lett.* **2008**, *18*, 1958.
12. Bakhite, E. A. *Phosphorus Sulfur Silicon* **2003**, *178*, 929.
13. Bompart, J.; Giral, L.; Malicorne, G.; Puygrenier, M. *Eur. J. Med. Chem.* **1987**, *22*, 139.
14. Moloney, G. P. *Molecules* **2001**, *6*, M203.
15. Bernardino, A. M. R.; Pinheiro, L. C. S.; Ferreira, V. F.; Azevedo, A. R.; Carneiro, J. W. deM.; Souza, T. M. L.; Frugulhetti, I. C. P. P. *Heterocycl. Commun.* **2004**, *10*, 407.
16. Bernardino, A. M. R.; Pinheiro, L. C. S.; Rodrigues, C. R.; Loureiro, N. I. V.; Castro, H. C.; Lanfredi-Rangel, A.; Sabatini-Lopes, J.; Borges, J. C.; Carvalho, J. M.; Romeiro, G. A.; Ferreira, V. F.; Frugulhetti, I. C. P. P.; Vannier-Santos, M. A. *Bioorg. Med. Chem.* **2006**, *14*, 5765.
17. Lipinski, C. A. *Annu. Rep. Med. Chem.* **1986**, *21*, 283.
18. Kier, L. B.; Hall, L. H. *Chem. Biodivers.* **2004**, *1*, 138.
19. Lipinski, C. A. *Drug Discov. Today* **2004**, *1*, 337.
20. Azevedo, A. R.; Ferreira, V. F.; Mello, H. M.; Leão-Ferreira, L. R.; Jabor, A. V.; Frugulhetti, I. C. P. P.; Pereira, H. S.; Moussatché, N.; Bernardino, A. M. R. *Heterocycl. Commun.* **2002**, *8*, 427.
21. Pinheiro, L. C. S.; Borges, J. C.; Oliveira, C. D.; Ferreira, V. F.; Romeiro, G. A.; Marques, I. P.; Abreu, P. A.; Frugulheti, I. C. P. P.; Rodrigues, C. R.; Albuquerque, M. G.; Castro, H. C.; Bernardino. A. M. R. *Arkivoc*, in press.
22. Tetko, I. V. *Drug Discov. Today* **2005**, *10*, 1497.
23. Szileigyl, G. *Arzneim.-Forsch.* **1984**, *35*, 1260.
24. Oliveira, C. G. T.; Miranda, F. F.; Ferreira, V. F.; Freitas, C. C.; Carballido Corrêa, J. M. L. C. D. *J. Braz. Chem. Soc.* **2001**, *12*, 339.
25. Cirne-Santos, C. C.; Teixeira, V. L.; Castello-Branco, L. R.; Frugulhetti, I. C.; Bou-Habib, D. C. *Planta Med.* **2006**, *72*, 295.